

Towards the theory of ferrimagnetism

This article has been downloaded from IOPscience. Please scroll down to see the full text article.

2008 J. Phys.: Condens. Matter 20 325219

(<http://iopscience.iop.org/0953-8984/20/32/325219>)

View [the table of contents for this issue](#), or go to the [journal homepage](#) for more

Download details:

IP Address: 129.252.86.83

The article was downloaded on 29/05/2010 at 13:48

Please note that [terms and conditions apply](#).

Towards the theory of ferrimagnetism

Naoum Karchev

Department of Physics, University of Sofia, 1164 Sofia, Bulgaria

E-mail: naoum@phys.uni-sofia.bg

Received 1 May 2008

Published 9 July 2008

Online at stacks.iop.org/JPhysCM/20/325219

Abstract

A two-sublattice ferrimagnet, with spin- s_1 operators \mathbf{S}_{1i} at the sublattice A site and spin- s_2 operators \mathbf{S}_{2i} at the sublattice B site, is considered. The magnon of the system, the transversal fluctuation of the total magnetization, is a complicate mixture of the transversal fluctuations of the sublattice A and B spins. As a result, the magnons' fluctuations suppress in a different way the magnetic orders of the A and B sublattices and one obtains two phases. At low temperature ($0, T^*$) the magnetic orders of the A and B spins contribute to the magnetization of the system, while at high temperature (T^*, T_N), the magnetic order of the spins with a weaker intra-sublattice exchange is suppressed by magnon fluctuations, and only the spins with stronger intra-sublattice exchange have non-zero spontaneous magnetization. The T^* transition is a transition between two spin-ordered phases in contrast to the transition from the spin-ordered state to the disordered state (T_N -transition). There is no additional symmetry breaking, and the Goldstone boson has a ferromagnetic dispersion in both phases. A modified spin-wave theory is developed to describe the two phases. All known Neel's anomalous $M(T)$ curves are reproduced, in particular that with 'compensation point'. The theoretical curves are compared with experimental ones for sulfo-spinel $\text{MnCr}_2\text{S}_{4-x}\text{Se}_x$ and rare earth iron garnets.

(Some figures in this article are in colour only in the electronic version)

1. Introduction

The notions of ferrimagnetism and ferrimagnetic materials were introduced by Neel [1] for materials in which spontaneous magnetization is a resultant of two or more components of non-parallel magnetic moments. Using a molecular field theory he predicted the nature of magnetization M versus temperature T . In Neel's theory anomalous $M(T)$ curves arise due to the fact that each of the magnetic moments approaches its own saturation value as a different function of temperature. In general there is nothing to limit the number of components. The simplest model consists of two alternating sublattices of unequal and antiparallel moments, with three molecular field coefficients utilized to describe the exchange field effects: one ferromagnetic coefficient for each sublattice and a third for the antiferromagnetic interaction. In many cases, the experimental curves are used to determine the molecular field coefficients. The most striking feature of the anomalous $M(T)$ curves is the possibility of 'compensation point', a temperature T_c at which the magnetic moments of the two sublattices are equal and opposite, so that the magnetization of the system is equal to zero $M(T_c) = 0$. The phenomenon of ferrimagnetism has been the subject of

extensive experimental investigation since its discovery. The phenomenological Neel's standpoint has been confirmed by many authors (see the review articles [2–6]).

The earliest application of spin waves to ferrimagnets was made by Kaplan [7] to calculate the dispersion ω_k for the spinel-type ferrite. For small wavevector \mathbf{k} he found a quadratic relation $\omega_k = D\mathbf{k}^2$, where D is a constant, as for ferromagnetism. To simplify the calculations Kaplan neglected the intra-sublattice exchange compared with the inter-sublattice one, so that the calculations do not correspond to any real ferrimagnet.

In the present paper I consider a two-sublattice ferrimagnet, with spin- s_1 operators \mathbf{S}_{1i} at the sublattice A site and spin- s_2 operators \mathbf{S}_{2i} at the sublattice B site. The Hamiltonian of the system is

$$H = -J_1 \sum_{\langle\langle ij \rangle\rangle_A} \mathbf{S}_{1i} \cdot \mathbf{S}_{1j} - J_2 \sum_{\langle\langle ij \rangle\rangle_B} \mathbf{S}_{2i} \cdot \mathbf{S}_{2j} + J \sum_{\langle ij \rangle} \mathbf{S}_{1i} \cdot \mathbf{S}_{2j} \quad (1.1)$$

where the sums are over all sites of a three-dimensional cubic lattice: $\langle i, j \rangle$ denotes the sum over the nearest neighbors, $\langle\langle i, j \rangle\rangle_A$ denotes the sum over the sites of the A sublattice, $\langle\langle i, j \rangle\rangle_B$ denotes the sum over the sites of the B sublattice. The first two terms describe the ferromagnetic Heisenberg

intra-sublattice exchange $J_1 > 0, J_2 > 0$, while the third term describes the inter-sublattice exchange which is antiferromagnetic $J > 0$.

The true magnons of a two-spin system are transversal fluctuations of the total magnetization which includes both the magnetization of the sublattice A and B spins. The magnon excitation is a complicated mixture of the transversal fluctuations of the sublattice A and B spins. As a result the magnons' fluctuations suppress, in different ways, the magnetic orders on the different sublattices and one obtains two phases. At low temperature ($0, T^*$) the magnetic orders of the A and B spins contribute to the magnetization of the system, while at high temperature (T^*, T_N) the magnetic order of the spins with a weaker intra-sublattice exchange is suppressed by magnon fluctuations, and only the spins with the stronger intra-sublattice exchange have non-zero spontaneous magnetization. At first sight the result that there is a temperature interval where a magnetic order is formed only by spins on one of the sublattices seems to be counterintuitive because the moment on the one of the sublattices builds an effective magnetic field, which due to inter-sublattice exchange interaction leads to a finite magnetization on the other sublattice. This is true in the classical limit. In the quantum case the spin-wave fluctuations suppress the A and B magnetic orders at different temperatures T^* and T_N as a result of a different interaction of magnons with the sublattices' spins. The T^* transition is a transition between two spin-ordered phases in contrast to the transition from the spin-ordered state to the disordered state (T_N -transition). There is no additional symmetry breaking and the Goldstone boson has a ferromagnetic dispersion in both phases.

A modified spin-wave theory is developed to describe the two phases. By means of this method of calculation the thermal variation of magnetization is calculated for three cases: ($s_1 > s_2$) $J_1 \gg J_2$, ($s_1 > s_2$) $J_2 \gg J_1$ and ($s_1 = s_2$) $J_1 \gg J_2$. All known Neel's anomalous $M(T)$ curves are reproduced including the curve with the famous 'compensation point' (second case).

An important issue is the experimental detection of the T^* transition. In the case when T^* is the temperature at which itinerant electrons start to form magnetic order the transition demonstrates itself through the change in the T dependence of resistivity. It is well known that the onset of magnetism in itinerant systems is accompanied with a strong anomaly in resistivity [8]. One expects the same phenomena when the itinerant electrons in ferrimagnets form magnetic order. There are experimental results which support the above interpretation of the T^* transition.

The paper is organized as follows. In section 2, a spin-wave theory of the model equation (1.1) is presented. The non-adequacy of the customary spin-wave theory for the description of the high temperature phase is shown. Section 3 is devoted to the development of a modified spin-wave theory. The calculations are accomplished for different choices of the model's parameters. The theoretical $M(T)$ curves are compared with experimental ones for sulfo-spinel $MnCr_2S_{4-x}Se_x$ [5] and rare earth iron garnets [2] and a satisfying coincidence is obtained. A summary in section 4 concludes the paper.

2. Spin-wave theory

To study a theory with Hamiltonian equation (1.1) it is convenient to introduce the Holstein–Primakoff representation for the spin operators

$$\begin{aligned} S_{1j}^+ &= S_{1j}^1 + iS_{1j}^2 = \sqrt{2s_1 - a_j^+ a_j} a_j \\ S_{1j}^- &= S_{1j}^1 - iS_{1j}^2 = a_j^+ \sqrt{2s_1 - a_j^+ a_j} \\ S_{1j}^3 &= s_1 - a_j^+ a_j \end{aligned} \quad (2.1)$$

when the sites j are from sublattice A, and

$$\begin{aligned} S_{2j}^+ &= S_{2j}^1 + iS_{2j}^2 = -b_j^+ \sqrt{2s_2 - b_j^+ b_j} \\ S_{2j}^- &= S_{2j}^1 - iS_{2j}^2 = -\sqrt{2s_2 - b_j^+ b_j} b_j \\ S_{2j}^3 &= -s_2 + b_j^+ b_j \end{aligned} \quad (2.2)$$

when the sites j are from sublattice B. The operators a_j^+, a_j and b_j^+, b_j satisfy the Bose commutation relations. In terms of the Bose operators and keeping only the quadratic terms the effective Hamiltonian equation (1.1) adopts the form

$$\begin{aligned} H &= s_1 J_1 \sum_{\langle\langle ij \rangle\rangle_A} (a_i^+ a_i + a_j^+ a_j - a_j^+ a_i - a_i^+ a_j) \\ &+ s_2 J_2 \sum_{\langle\langle ij \rangle\rangle_B} (b_i^+ b_i + b_j^+ b_j - b_j^+ b_i - b_i^+ b_j) \\ &+ \sum_{\langle ij \rangle} [s_1 J b_j^+ b_j + s_2 J a_i^+ a_i - J \sqrt{s_1 s_2} (a_i^+ b_j^+ + a_i b_j)]. \end{aligned} \quad (2.3)$$

To proceed one rewrites the Hamiltonian in the momentum space representation

$$H = \sum_{k \in B_r} [\varepsilon_k^a a_k^+ a_k + \varepsilon_k^b b_k^+ b_k - \gamma_k (a_k^+ b_k^+ + b_k a_k)], \quad (2.4)$$

where the wavevector k runs over the reduced first Brillouin zone B_r of a cubic lattice. The dispersions are given by equalities

$$\begin{aligned} \varepsilon_k^a &= 4s_1 J_1 \varepsilon_k + 6s_2 J \\ \varepsilon_k^b &= 4s_2 J_2 \varepsilon_k + 6s_1 J \end{aligned} \quad (2.5)$$

with

$$\begin{aligned} \varepsilon_k &= 6 - \cos(k_x + k_y) - \cos(k_x - k_y) - \cos(k_x + k_z) \\ &- \cos(k_x - k_z) - \cos(k_y + k_z) - \cos(k_y - k_z) \end{aligned} \quad (2.6)$$

and

$$\gamma_k = 2J \sqrt{s_1 s_2} (\cos k_x + \cos k_y + \cos k_z). \quad (2.7)$$

To diagonalize the Hamiltonian one introduces new Bose fields $\alpha_k, \alpha_k^+, \beta_k, \beta_k^+$ by means of the transformation

$$\begin{aligned} a_k &= u_k \alpha_k + v_k \beta_k^+ & a_k^+ &= u_k \alpha_k^+ + v_k \beta_k \\ b_k &= u_k \beta_k + v_k \alpha_k^+ & b_k^+ &= u_k \beta_k^+ + v_k \alpha_k \end{aligned} \quad (2.8)$$

where the coefficients of the transformation u_k and v_k are real functions of the wavevector k

$$u_k = \frac{1}{2} \left(\frac{\varepsilon_k^a + \varepsilon_k^b}{\sqrt{(\varepsilon_k^a + \varepsilon_k^b)^2 - 4\gamma_k^2}} + 1 \right) \quad (2.9)$$

$$v_k = \text{sgn}(\gamma_k) \sqrt{\frac{1}{2} \left(\frac{\varepsilon_k^a + \varepsilon_k^b}{\sqrt{(\varepsilon_k^a + \varepsilon_k^b)^2 - 4\gamma_k^2}} - 1 \right)}.$$

The transformed Hamiltonian adopts the form

$$H = \sum_{k \in B_r} \left(E_k^\alpha \alpha_k^+ \alpha_k + E_k^\beta \beta_k^+ \beta_k + E_k^0 \right), \quad (2.10)$$

with new dispersions

$$E_k^\alpha = \frac{1}{2} \left[\sqrt{(\varepsilon_k^a + \varepsilon_k^b)^2 - 4\gamma_k^2} - \varepsilon_k^b + \varepsilon_k^a \right] \quad (2.11)$$

$$E_k^\beta = \frac{1}{2} \left[\sqrt{(\varepsilon_k^a + \varepsilon_k^b)^2 - 4\gamma_k^2} + \varepsilon_k^b - \varepsilon_k^a \right]$$

and vacuum energy

$$E_k^0 = \frac{1}{2} \left[\sqrt{(\varepsilon_k^a + \varepsilon_k^b)^2 - 4\gamma_k^2} - \varepsilon_k^b - \varepsilon_k^a \right]. \quad (2.12)$$

For all values of k , $\sqrt{(\varepsilon_k^a + \varepsilon_k^b)^2 - 4\gamma_k^2} \geq |\varepsilon_k^b - \varepsilon_k^a|$, and the dispersions are nonnegative $E_k^\alpha \geq 0$, $E_k^\beta \geq 0$.

For definiteness I choose $s_1 > s_2$. With these parameters, the β_k -boson is a gapped excitation with gap

$$E_0^\beta = 6J(s_1 - s_2), \quad (2.13)$$

while the α_k -boson is the long-range (magnon) excitation in the two-spin system. Near the zero wavevector

$$E_k^\alpha \approx \rho k^2 \quad (2.14)$$

where the spin-stiffness constant is

$$\rho = \frac{8s_1^2 J_1 + 8s_2^2 J_2 + 2s_1 s_2 J}{s_1 - s_2}. \quad (2.15)$$

The spontaneous magnetization of the system M is a sum of the spontaneous magnetization on the two sublattices $M = M^A + M^B$, where

$$M^A = \langle S_{1j}^3 \rangle \quad j \text{ is from sublattice A} \quad (2.16)$$

$$M^B = \langle S_{2j}^3 \rangle \quad j \text{ is from sublattice B.}$$

In terms of the Holstein–Primakoff bosons (a_k and b_k) the magnetization adopts the form

$$M^A = s_1 - \frac{1}{N} \sum_{k \in B_r} \langle a_k^+ a_k \rangle \quad (2.17)$$

$$M^B = -s_2 + \frac{1}{N} \sum_{k \in B_r} \langle b_k^+ b_k \rangle$$

where $N_A = N_B = N$ are the numbers of sites on sublattices A and B. Finally one can rewrite M^A and M^B in terms of the α_k (α_k^+) and β_k (β_k^+) excitations

$$M^A = s_1 - \frac{1}{N} \sum_{k \in B_r} [u_k^2 \langle \alpha_k^+ \alpha_k \rangle + v_k^2 \langle \beta_k \beta_k^+ \rangle] \quad (2.18)$$

$$M^B = -s_2 + \frac{1}{N} \sum_{k \in B_r} [u_k^2 \langle \beta_k^+ \beta_k \rangle + v_k^2 \langle \alpha_k \alpha_k^+ \rangle].$$

Then, the magnetization of the system adopts the form

$$M = s_1 - s_2 - \frac{1}{N} \sum_{k \in B_r} [\langle \alpha_k^+ \alpha_k \rangle - \langle \beta_k^+ \beta_k \rangle]. \quad (2.19)$$

In equations (2.18) and (2.19)

$$\langle \alpha_k^+ \alpha_k \rangle = \frac{1}{e^{E_k^\alpha/T} - 1}, \quad \langle \alpha_k \alpha_k^+ \rangle = 1 + \langle \alpha_k^+ \alpha_k \rangle \quad (2.20)$$

$$\langle \beta_k^+ \beta_k \rangle = \frac{1}{e^{E_k^\beta/T} - 1}, \quad \langle \beta_k \beta_k^+ \rangle = 1 + \langle \beta_k^+ \beta_k \rangle.$$

We consider a theory with Hamiltonian equation (1.1), where the sums are over all sites of a three-dimensional cubic lattice with space size $a = 1$. The two equivalent sublattices A and B are face centered cubic (fcc) lattices with space size $2a = 2$. The coordinates k_x, k_y, k_z of the wavevector k are coordinates in the basis $\hat{x}, \hat{y}, \hat{z}$, which are primitive vectors of the cubic lattice. To implement the integrations over the wavevector it is more convenient to switch to coordinates q_1, q_2, q_3 in the basis $\hat{A}, \hat{B}, \hat{C}$, which are primitive vectors of the reciprocal lattice, to the fcc lattice with space size equal to 2.

$$\hat{A} = \pi (\hat{x} + \hat{y} - \hat{z})$$

$$\hat{B} = \pi (-\hat{x} + \hat{y} + \hat{z}) \quad (2.21)$$

$$\hat{C} = \pi (\hat{x} - \hat{y} + \hat{z}).$$

To that end we utilize the transformation

$$k_x = \pi q_1 - \pi q_2 + \pi q_3$$

$$k_y = \pi q_1 + \pi q_2 - \pi q_3 \quad (2.22)$$

$$k_z = -\pi q_1 + \pi q_2 + \pi q_3.$$

The Jacobian of the transformation is equal to $4\pi^3$, so that $d^3k/(2\pi)^3 = d^3q/2$. When the wavevector k runs over the reduced Brillouin zone $k \in B_r$, the new vector runs over the cube $0 \leq q_l \leq 1$. Finally we introduce the more convenient coordinates $p_1 = \pi q_1; p_2 = \pi q_2; p_3 = \pi q_3$. They run over the interval $[0, \pi]$ and $d^3k/(2\pi)^3 = d^3p/2\pi^3$. In terms of the new coordinates the functions of the wavevector (2.6) and (2.7) adopts the form

$$\varepsilon_p = 6 - \cos(2p_1) - \cos(2p_2) - \cos(2p_3)$$

$$- \cos 2(p_1 - p_2) - \cos 2(p_1 - p_3) - \cos 2(p_2 - p_3)$$

$$\gamma_p = 2J\sqrt{s_1 s_2} [\cos(-p_1 + p_2 + p_3) + \cos(p_1 - p_2 + p_3)$$

$$+ \cos(p_1 + p_2 - p_3)]. \quad (2.23)$$

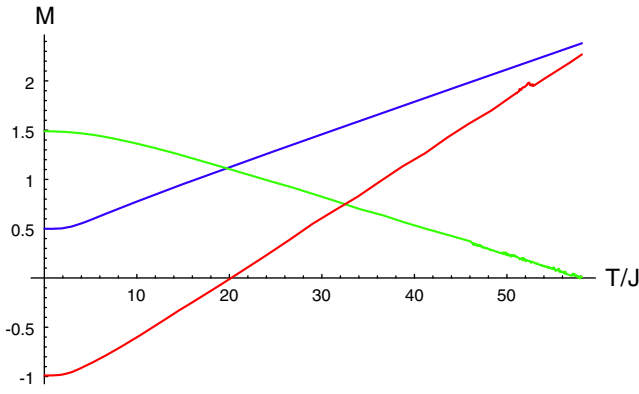


Figure 1. Temperature dependence of the ferromagnetic moments: M (blue line)—the magnetization of the system, M^A (green line)—sublattice A magnetization, M^B (red line)—sublattice B magnetization for parameters $s_1 = 1.5$, $s_2 = 1$, $J_1/J = 0.47$ and $J_2/J = 0.005$: spin-wave theory.

The magnon excitation- α_k in the effective theory equation (2.10) is a complicated mixture of the transversal fluctuations of the A and B spins. As a result the magnons' fluctuations suppress in a different way the magnetic order on sublattices A and B. Quantitatively this depends on the coefficients u_k and v_k in equations (2.18). The magnetization depends on the dimensionless temperature T/J and dimensionless parameters $s_1, s_2, J_1/J$ and J_2/J . For parameters $s_1 = 1.5, s_2 = 1, J_1/J = 0.47$ and $J_2/J = 0.005$ the functions $M(T/J), M^A(T/J)$ and $M^B(T/J)$ are depicted in figure 1. The upper (green) line is the sublattice A magnetization, the bottom (red) line is the sublattice B magnetization and the middle (blue) line is the magnetization of the system. The figure shows that the magnetic order on sublattice B (red line) is suppressed first, at temperature $T^*/J = 20$. Once suppressed, the magnetic order can not be restored at temperatures above T^* because of the increasing effect of magnon fluctuations. Hence, the sublattice B magnetization should be zero above T^* . It is evident from figure 1, that this is not the result within customary spin-wave theory.

3. Modified spin-wave theory

To solve the problem we use the idea on description of paramagnetic phase of 2D ferromagnets ($T > 0$) by means of modified spin-wave theory [9, 10]. In the simplest version the spin-wave theory is modified by introducing a new parameter which forces the magnetization of the system to be equal to zero in the paramagnetic phase.

We consider the two-sublattice system and force the magnetic moments on the two sublattices to be equal to zero in the paramagnetic phase, we also introduce two parameters λ_1 and λ_2 . The new Hamiltonian is obtained from the old one adding two new terms to the Hamiltonian equation (1.1)

$$\hat{H} = H - \sum_{i \in A} \lambda_1 S_{1i}^3 + \sum_{i \in B} \lambda_2 S_{2i}^3. \quad (3.1)$$

In momentum space the new Hamiltonian adopts the form

$$\hat{H} = \sum_{k \in B_r} [\hat{\varepsilon}_k^a a_k^+ a_k + \hat{\varepsilon}_k^b b_k^+ b_k - \gamma_k (b_k a_k + b_k^+ a_k^+)] \quad (3.2)$$

where the new dispersions are

$$\hat{\varepsilon}_k^a = \varepsilon_k^a + \lambda_1, \quad \hat{\varepsilon}_k^b = \varepsilon_k^b + \lambda_2. \quad (3.3)$$

Utilizing the same transformation equation (2.8) with parameters

$$\hat{u}_k = \sqrt{\frac{1}{2} \left(\frac{\hat{\varepsilon}_k^a + \hat{\varepsilon}_k^b}{\sqrt{(\hat{\varepsilon}_k^a + \hat{\varepsilon}_k^b)^2 - 4\gamma_k^2}} + 1 \right)}$$

$$\hat{v}_k = \text{sgn}(\gamma_k) \sqrt{\frac{1}{2} \left(\frac{\hat{\varepsilon}_k^a + \hat{\varepsilon}_k^b}{\sqrt{(\hat{\varepsilon}_k^a + \hat{\varepsilon}_k^b)^2 - 4\gamma_k^2}} - 1 \right)}$$
(3.4)

one obtains the Hamiltonian in diagonal form

$$\hat{H} = \sum_{k \in B_r} \left(\hat{E}_k^\alpha \alpha_k^+ \alpha_k + \hat{E}_k^\beta \beta_k^+ \beta_k + \hat{E}_k^0 \right), \quad (3.5)$$

where

$$\hat{E}_k^\alpha = \frac{1}{2} \left[\sqrt{(\hat{\varepsilon}_k^a + \hat{\varepsilon}_k^b)^2 - 4\gamma_k^2} - \hat{\varepsilon}_k^b + \hat{\varepsilon}_k^a \right]$$

$$\hat{E}_k^\beta = \frac{1}{2} \left[\sqrt{(\hat{\varepsilon}_k^a + \hat{\varepsilon}_k^b)^2 - 4\gamma_k^2} + \hat{\varepsilon}_k^b - \hat{\varepsilon}_k^a \right]$$

$$\hat{E}_k^0 = \frac{1}{2} \left[\sqrt{(\hat{\varepsilon}_k^a + \hat{\varepsilon}_k^b)^2 - 4\gamma_k^2} - \hat{\varepsilon}_k^b - \hat{\varepsilon}_k^a \right]. \quad (3.6)$$

We have to make some assumptions for the parameters λ_1 and λ_2 to ensure the correct definition of the Bose theory. For that purpose it is convenient to represent the parameters λ_1 and λ_2 in the form

$$\lambda_1 = 6J s_2 \mu_1 - 6J s_2, \quad \lambda_2 = 6J s_1 \mu_2 - 6J s_1. \quad (3.7)$$

In terms of the new parameters μ_1 and μ_2 the dispersions $\hat{\varepsilon}_k^a$ and $\hat{\varepsilon}_k^b$ adopt the form

$$\hat{\varepsilon}_k^a = 4s_1 J_1 \varepsilon_k + 6J s_2 \mu_1$$

$$\hat{\varepsilon}_k^b = 4s_2 J_2 \varepsilon_k + 6J s_1 \mu_2. \quad (3.8)$$

We assume μ_1 and μ_2 to be positive ($\mu_1 > 0, \mu_2 > 0$), then $\hat{\varepsilon}_k^a > 0$ and $\hat{\varepsilon}_k^b > 0$ for all values of the wavevector k . The Bose theory is well defined if the square-roots in equation (3.6) are well defined and $E_k^\alpha \geq 0, E_k^\beta \geq 0$. This is true if

$$\mu_1 \mu_2 \geq 1. \quad (3.9)$$

The β_k -excitation is gapped ($E_k^\beta > 0$) for all values of parameters μ_1 and μ_2 which satisfy equation (3.9). The α -excitation is gapped if $\mu_1 \mu_2 > 1$, but in the particular case

$$\mu_1 \mu_2 = 1 \quad (3.10)$$

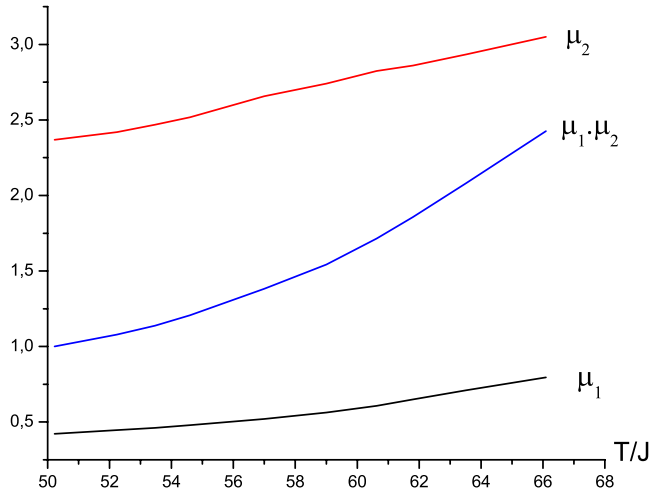


Figure 2. The solution of the system of equation (3.13) $\mu_1(T/J)$, $\mu_2(T/J)$ and $\mu_1(T/J) \cdot \mu_2(T/J)$ for parameters $s_1 = 1.5$, $s_2 = 1$, $J_1/J = 0.47$ and $J_2/J = 0.005$.

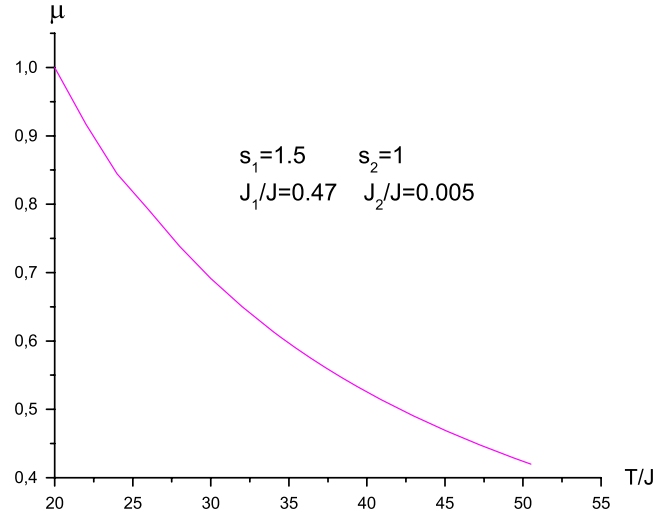


Figure 3. Temperature dependence of μ for T between T^* and T_N and parameters $s_1 = 1.5$, $s_2 = 1$, $J_1/J = 0.47$ and $J_2/J = 0.005$.

$\hat{E}_0^\alpha = 0$, and near the zero wavevector

$$\hat{E}_k^\alpha \approx \hat{\rho} k^2 \quad (3.11)$$

with spin-stiffness constant

$$\hat{\rho} = \frac{8(s_2^2 J_2 \mu_1 + s_1^2 J_1 \mu_2) + 2s_1 s_2 J}{(s_1 \mu_2 - s_2 \mu_1)}. \quad (3.12)$$

In the particular case of equation (3.10) the α_k -boson is the long-range excitation (magnon) in the system.

3.1. $s_1 > s_2$ and $J_1 \gg J_2$

We introduced the parameters λ_1 and λ_2 (μ_1, μ_2) to force the spontaneous magnetization on the sublattices A and B to be equal to zero. We find the parameters μ_1 and μ_2 , as functions of temperature, solving the system of two equations $M^A = 0$, $M^B = 0$

$$\begin{aligned} s_1 - \frac{1}{N} \sum_{k \in B_r} [\hat{u}_k^2 \langle \alpha_k^+ \alpha_k \rangle + \hat{v}_k^2 \langle \beta_k \beta_k^+ \rangle] &= 0 \\ -s_2 + \frac{1}{N} \sum_{k \in B_r} [\hat{u}_k^2 \langle \beta_k^+ \beta_k \rangle + \hat{v}_k^2 \langle \alpha_k \alpha_k^+ \rangle] &= 0 \end{aligned} \quad (3.13)$$

where the coefficients \hat{u}_k and \hat{v}_k are given by equations (3.4) and the Bose functions (2.20) are defined with dispersions \hat{E}_k^α and \hat{E}_k^β . The solutions $\mu_1(T/J)$ and $\mu_2(T/J)$ depend on the parameters $s_1, s_2, J_1/J$ and J_2/J . For $s_1 = 1.5, s_2 = 1, J_1/J = 0.47$ and $J_2/J = 0.005$ they are depicted in figure 2.

The upper (red) line is $\mu_2(T/J)$, the bottom (black) line is $\mu_1(T/J)$ and the middle (blue) line is the product $\mu_1(T/J) \cdot \mu_2(T/J)$. The numerical calculations show that for high enough temperature $\mu_2 > 1, 1 > \mu_1 > 0$ and $\mu_1 \cdot \mu_2 > 1$. Hence α_k and β_k excitations are gapped. When the temperature decreases μ_2 decreases remaining larger than one, μ_1 decreases as well remaining positive, and the product

$\mu_1 \cdot \mu_2$ decreases remaining larger than one. At temperature $T_N/J = 50.22$ one obtains $\mu_1 = 0.422, \mu_2 = 2.368$ and therefore $\mu_1 \cdot \mu_2 = 1$. Hence, at T_N a long-range excitation (magnon) emerges in the spectrum which means that T_N is the Neel temperature.

Below the Neel temperature the spectrum contains magnon excitations, thereupon $\mu_1 \cdot \mu_2 = 1$. It is convenient to set

$$\mu_1 = \mu, \quad \mu_2 = 1/\mu. \quad (3.14)$$

In the ordered phase magnon excitations are the origin of suppression of the magnetization. Near zero temperature their contribution is small and at zero temperature they are close to s_1 and s_2 . Increasing the temperature magnon fluctuations suppress the magnetization. For the chosen parameters they first suppress the sublattice B magnetization at T^* ($M^A(T^*) > 0$). Once suppressed, the magnetic moment of sublattice B spins can not be restored by increasing the temperature above T^* . To formulate this mathematically, we modify the spin-wave theory introducing the parameter μ equation (3.14). Below T^* $\mu = 1$, or in terms of λ parameters $\lambda_1 = \lambda_2 = 0$, which reproduces the customary spin-wave theory. Increasing the temperature above T^* the magnetic moment of the sublattice B spins should be zero. This is why we impose the condition $M^B(T) = 0$ if $T > T^*$. For temperatures above T^* the parameter μ is a solution of this equation. The function $\mu(T/J)$ is depicted in figure 3. Increasing the temperature above T^* , $\mu(T/J)$ decreases from $\mu(T^*/J) = 1$ to $\mu(T_N/J) = \mu_1(T_N/J) = 0.422$.

Next, one utilizes the so obtained function $\mu(T/J)$ to calculate the sublattice A magnetization as a function of the temperature. Above T^* , M^A is equal to the magnetization of the system. The magnetic moments of the sublattice A and B spins, as well as the magnetization of the system, as a function of the temperature are depicted in figure 4 for parameters $s_1 = 1.5, s_2 = 1, J_1/J = 0.47, J_2/J = 0.005$.

To compare the theoretical results and the experimental $M(T)$ curves one has, first of all, to interpret adequately the

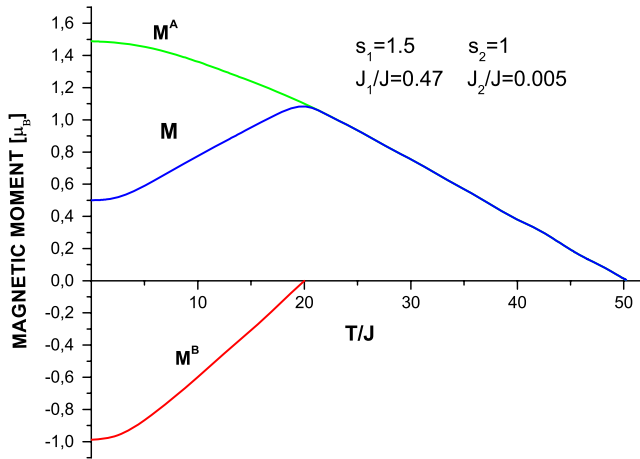


Figure 4. Temperature dependence of the ordered moments: M (blue line)—the magnetic moment of the system, M^A (green line)—sublattice A magnetic moment, M^B (red line)—sublattice B magnetic moment for parameters $s_1 = 1.5$, $s_2 = 1$, $J_1/J = 0.47$ and $J_2/J = 0.005$: modified spin-wave theory.

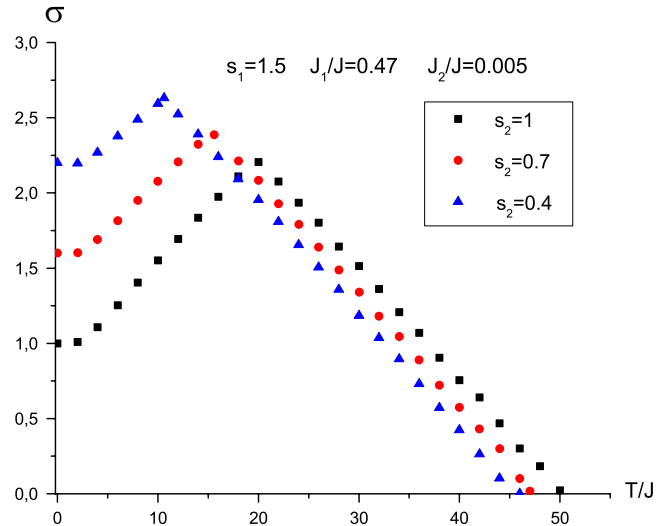


Figure 5. The magnetization, in Bohr magnetons, per lattice site $\sigma = 2(M^A + M^B)$ for $s_1 = 1.5$, $J_1/J = 0.47$, $J_2/J = 0.005$ and $s_2 = 1; 0.7; 0.4$.

measurements. The magnetic moments in some materials are close to the ‘spin only’ value $2 \mu_B S$ and the sublattice spins s_1 and s_2 can be obtained from the experimental curves. I consider the system $\text{MnCr}_2\text{S}_{4-x}\text{Se}_x$. It has been investigated by measurements of the magnetization at 15.3 kOe as a function of temperature (figure 94 in [5]). The maximum in the magnetization versus temperature curve, which is typical of MnCr_2S_4 ($x = 0$), increases when x increases, and disappears at $x = 0.5$. The Neel temperature decreases from 74 K at $x = 0$ to 56 K at $x = 2$. The authors’ conclusion is that the observed change of the magnetic properties is attributed to a decrease of the strength of the negative $\text{Mn}^{2+}\text{-Cr}^{3+}$ superexchange interaction with increasing Se concentration.

As follows from the present theory (see figure 4 middle blue line) the maximum of the magnetization is at T^* . Above T^* the magnetization of the system is equal to the magnetization of sublattice A spins. If we extrapolate this curve below T^* down to zero temperature we will obtain a value close to $2s_1 \mu_B$, where s_1 is the spin of the sublattice A spin operators. The figure shows that extrapolations give one and the same result for all values of x . One can accept the fact that the Se concentration does not influence the value of sublattice A spin and $s_1 = 1.5$.

Below T^* the magnetization is a sum of the sublattice A and B magnetization. Hence, the magnetization at zero temperature is equal to $2(s_1 - s_2) \mu_B$. Therefore, one can determine the sublattice B spin s_2 . The important conclusion is that the effective sublattice B spin s_2 decreases with increasing Se concentration. The dimensionless magnetization (in Bohr magnetons) per lattice site $\sigma = 2(M^A + M^B)$ is calculated for $s_1 = 1.5$, $J_1/J = 0.47$, $J_2/J = 0.005$ and $s_2 = 1; 0.7; 0.4$. The curves are depicted in figure 5. The figure shows that the present calculations capture the essential features of the system; increasing the Se concentration (decreasing s_2) leads to a decrease of Neel temperature, the T^* temperature decreases too, and the maximum of the magnetization $\sigma(T^*)$ increases.

3.2. $s_1 > s_2$ and $J_2 \gg J_1$

Next I consider the case when the sublattice A spin s_1 is larger than the sublattice B spin s_2 but the intra-sublattice exchange constant J_1 is much smaller than the intra-sublattice B exchange constant J_2 . Increasing the temperature, the magnon fluctuations suppress the magnetic order and the sublattice A magnetization decreases faster than the sublattice B magnetization. There is a temperature T_c at which the magnetization of the system is zero $M(T_c) = 0$ (the compensation point). Increasing the temperature above T_c the sublattice A magnetization becomes equal to zero at T^* . Above this temperature the sublattice A magnetization should be kept equal to zero and one utilizes the modified spin-wave theory to calculate the magnetization of the system which is equal to the sublattice B magnetization. The magnetization curves $M^A(T/J)$, $M^B(T/J)$ and $M(T/J)$ are depicted in figure 6 for parameters $s_1 = 18$, $s_2 = 3$, $j_1 = J_1/J = 0.005$ and $j_2 = J_2/J = 1$.

To compare the theoretical results with experimental ones I address the magnetization–temperature curves of rare earth iron garnets. When a rare earth ion, such as Gd^{3+} through Yb^{3+} , is present instead of a diamagnetic ion, such as Y^{3+} in Yttrium Iron Garnet, it is found that the magnetization as a function of temperature shows compensation points, i.e. the temperatures at which the spontaneous magnetization is zero (figure 5 [2]). I use the ‘spin only’ value for the magnetization, and the sublattices’ spins are considered as effective parameters to be determined from the experimental curves. The magnetization, in Bohr magnetons, per lattice site $\sigma = 2|M^A + M^B|$ are depicted in the figures. T^* is the temperature at which the sublattice A magnetization becomes equal to zero (black line figure 6), and hence the magnetization is minimal (blue line figure 6); in the case of the $\sigma(T)$ curves T^* is the temperature, above the compensation point, at which $\sigma(T^*)$ is maximal. The magnetization above T^* is equal to the sublattice B magnetization. To assess the value of the sublattice B spin s_2 ,

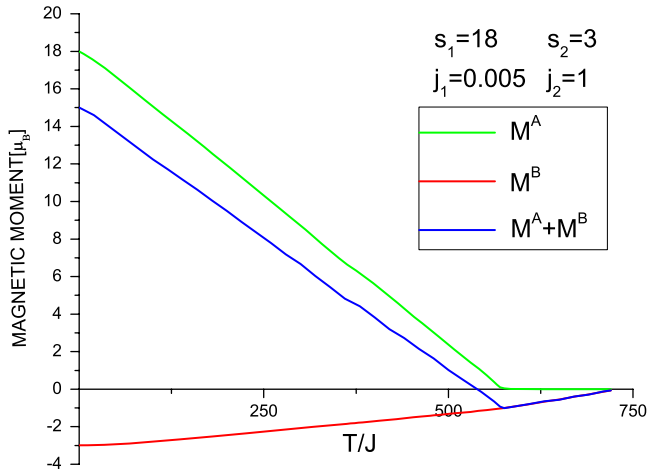


Figure 6. The magnetization curves: $M^A(T/J)$ —upper (green) line, $M^B(T/J)$ —bottom (red) line, $M(T/J)$ —middle (blue) line for parameters $s_1 = 18$, $s_2 = 3$, $j_1 = J_1/J = 0.005$ and $j_2 = J_2/J = 1$: modified spin-wave theory.

one has to extrapolate the curve to zero temperature. Then the spin s_1 can be obtained from the zero temperature of the magnetization $2(s_1 - s_2)\mu_B$. The experimental curves (figure 5 [2]) show that the value of $\sigma(T^*)$ is different for different rare earth ions, and hence the effective spin s_2 is different for different rare earths. It is smaller for gadolinium, increases for terbium, dysprosium, holmium, and is higher for ytterbium. At the same time the temperature T^* decreases, which means that sublattice B intra-exchange constant J_2 decreases. The magnetization $\sigma = 2|M^A + M^B|$ for two choices of the parameters are depicted in figure 7: black squares— $s_1 = 18$, $s_2 = 3$, $j_1 = J_1/J = 0.005$, $j_2 = J_2/J = 1$ and red circles— $s_1 = 18$, $s_2 = 6$, $j_1 = J_1/J = -0.05$, $j_2 = J_2/J = 0.15$. The negative sign of J_1 in the second group of parameters is chosen to reproduce the shape of the experimental curves. One can do better fitting, with positive constants J_2 for all rare earths, accounting for magnon scattering processes.

3.3. $s_1 = s_2$ and $J_1 \gg J_2$

Finally I consider a theory with parameters $s_1 = s_2 = s$ and $J_1 \gg J_2$. It is more correct to think of this case as a generalization of antiferromagnetism. The system has two magnons with dispersions E_k^α and E_k^β . Near the zero wavevector the dispersions' asymptotic is as in the antiferromagnetic case

$$E_k^\alpha \approx v_s |\mathbf{k}|, \quad E_k^\beta \approx v_s |\mathbf{k}| \quad (3.15)$$

with spin-wave velocity

$$v_s = 2s\sqrt{12J_1J + 12J_2J + 3J^2}. \quad (3.16)$$

As a result, at zero temperature, and near the zero temperature, one observes a compensation of sublattice A and B magnetization and the magnetization of the system is zero. The difference of the dispersions is

$$E_k^\alpha - E_k^\beta = 4s(J_1 - J_2)\varepsilon_k \approx 8s(J_1 - J_2)\mathbf{k}^2, \quad (3.17)$$

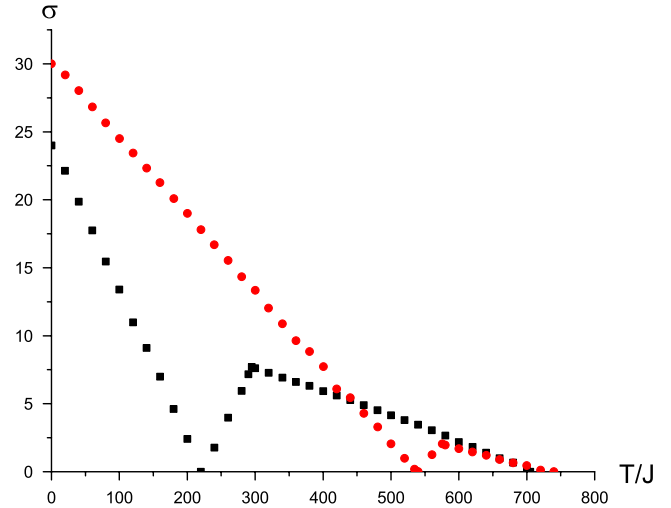


Figure 7. The magnetization $\sigma = 2|M^A + M^B|$ as a function of T/J : black squares— $s_1 = 18$, $s_2 = 3$, $J_1/J = 0.005$, $J_2/J = 1$, red circles— $s_1 = 18$, $s_2 = 6$, $J_1/J = -0.05$, $J_2/J = 0.15$.

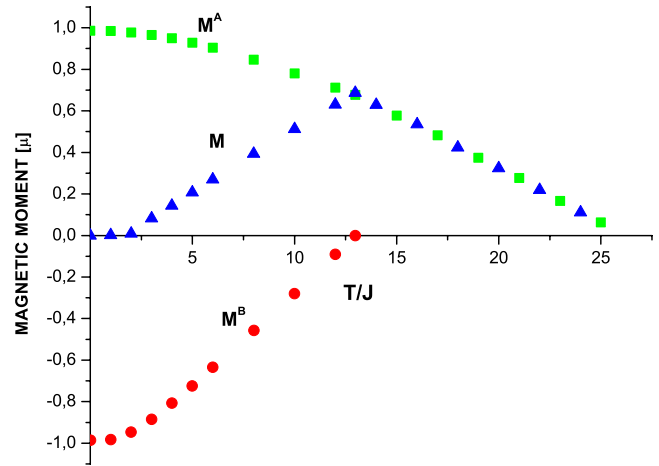


Figure 8. The magnetization curves: $M^A(T/J)$ —green squares, $M^B(T/J)$ —red circles, $M(T/J)$ —blue triangles for parameters $s_1 = 1$, $s_2 = 1$, $J_1/J = 0.47$ and $J_2/J = 0.005$: modified spin-wave theory.

therefore increasing the temperature one obtains non-compensation of sublattice A and B magnetization. The magnon fluctuations first suppress the sublattice B magnetization at temperature T^* . Above this temperature only sublattice A contributes to the magnetization. The magnetization curves $M^A(T/J)$, $M^B(T/J)$ and $M(T/J)$ are depicted in figure 8 for parameters $s_1 = 1$, $s_2 = 1$, $J_1/J = 0.47$ and $J_2/J = 0.005$. The magnetization–temperature curve (blue triangles) reproduces Neel's anomaly.

4. Summary

In summary, I have calculated the magnetization as a function of temperature for two-sublattice ferrimagnet. The anomalous temperature dependence of the magnetization, predicted by Neel, is reproduced, and the shape of the theoretical curves

satisfactorily coincides with the experimental ones. The most important difference between Neel's theory and the present modified spin-wave theory is that Neel's calculations predict a temperature T_N at which both the sublattice A and B magnetizations become equal to zero. The modified spin-wave theory predicts two phases: at low temperatures ($0, T^*$) the magnetic orders of the two sublattices contribute to the magnetization of the system, while at high temperatures (T^*, T_N) only one of the sublattices, that with a stronger intra-sublattice exchange, has non-zero spontaneous magnetization. It is important to stress that despite the fact that only one of the spins contributes to the magnetic order at high temperatures $T^* < T < T_N$ this is not a ferromagnetic phase. This is a ferrimagnetic phase because the magnon of the system is a mixture of the transversal fluctuations of the two spins.

Two ferromagnetic phases were theoretically predicted, very recently, in spin-Fermion systems, which obtain their magnetic properties from a system of localized magnetic moments being coupled to conducting electrons [11]. At the characteristic temperature T^* , the magnetization of itinerant electrons becomes zero, and the high temperature ferromagnetic phase ($T^* < T < T_C$) is a phase where only localized electrons give a contribution to the magnetization of the system. An anomalous increase of magnetization below T^* is obtained in good agreement with experimental measurements of the ferromagnetic phase of UGe_2 [12]. The results of the present paper and the previous one [11] suggest that the T^* transition from a magnetic phase to another magnetic phase is a generic feature of the two-spin systems. The additional phase transition demonstrates itself through the anomalous temperature variation of the spontaneous magnetization. Another way is possible, to experimentally identify the transition, if T^* is the temperature at which the itinerant electrons in the system start to form a magnetic moment. We know from itinerant ferromagnetism that the transition is observed through the change in the temperature dependence of resistivity. The most prominent example is the spinel Fe_3O_4 . It has been extensively investigated and the most striking feature is the Verwey transition [13]. At a relatively low temperature $T_V = 100\text{--}120$ K the magnetization abruptly changes slope, and the conductivity has an anomalous behavior. Many decades of research on Fe_3O_4 have led to the view [14–16] that the spinel is a two-sublattice system with three spins. The Fe_A^{3+} and Fe_B^{3+} ions are associated with localized spins on sublattices A and B, while Fe_B^{2+} ions are associated with itinerant electrons on sublattice B. With this in mind one can interpret the Neel temperature T_N as the temperature at which the magnetic moment of Fe_B^{3+} ions sets in, while the Verwey temperature T_V is the temperature at which the magnetic moment of Fe_A^{3+} ions sets in. There are two phases: a low temperature phase where Fe_A^{3+} and Fe_B^{3+} ions contribute to the magnetization and a high temperature phase where only Fe_B^{3+} ions contribute to the magnetization. The itinerant electrons interact with the localized spins, which leads to a renormalization of the hopping parameter. The renormalization is different at low and high temperatures because it depends on the orientation of the magnetic orders. As a result the transport properties are different at high and low temperatures.

Another example is the manganese vanadium oxide spinel MnV_2O_4 [17]. The A site of the spinel is occupied by the Mn^{2+} ion, which is in the $3d^5$ high-spin configuration with quenched orbital angular momentum, which can be regarded as a simple $s = 5/2$ spin. The B site is occupied by the V^{3+} ion, which takes the $3d^2$ high-spin configuration in the triply degenerate t_{2g} orbital, and has orbital degrees of freedom. Because of the strong spin-orbital interaction it is convenient to consider jj coupling with $\mathbf{J}^A = \mathbf{S}^A$ and $\mathbf{J}^B = \mathbf{L}^B + \mathbf{S}^B$. The sublattice A total angular momentum is $j_A = s_A = 5/2$, while the sublattice B total angular momentum is $j_B = l_B + s_B$ with $l_B = 1$ and $s_B = 3/2$. Finally, the g -factor for the sublattice A is $g_A = 2$, and the atomic value of the g_B is $g_B = 1.6$. Then, the zero temperature value of the magnetization is $\sigma(0) = 2\frac{5}{2} - 1.6\frac{5}{2}$.

The measurements of the magnetization as a function of temperature [17–19] show that the set in of magnetic order is due to Mn localized electrons at the Neel temperature $T_N = 56$ K [17]. The vanadium electrons start to form magnetic moments at $T^* = 48$ K. An evidence for this is the abrupt decrease of magnetization below T^* , which also indicates that the magnetic order of vanadium electrons is antiparallel with the order of Mn electrons. When the temperature approaches zero the magnetization goes to zero too, which indicates that the real value of g_B is not the atomic one but $g_B \approx 2$. The deviation is due to the anisotropy which increases the g_B -factor.

The above analysis concerns the ZFC magnetization. For samples cooled in a field (FC magnetization) the field leads to formation of a single domain and, in addition, increases the chaotic order of the spontaneous magnetization of the vanadium electrons, which is antiparallel to it. As a result the average value of the vanadium magnetic order decreases and does not compensate the Mn magnetic order ($\sigma(0) \neq 0$). The magnetization curves depend on the applied field, and does not go to zero. For a larger field the (FC) curve increases when the temperature decreases below the Neel temperature. It has a maximum at the same temperature $T^* < T_N$ and, what is the difference, it has a minimum at $T_1^* < T^*$. Below T_1^* the magnetization increases monotonically when the temperature approaches zero. As in the ZFC case, T^* is the temperature at which the vanadium electrons start to form magnetic order. Now, because of the strong field, the vanadium bands are split and part of the magnetic orders are reoriented to be parallel to the field and magnetic order of the Mn electrons. As a result, when $T_1^* < T < T^*$ only one of the vanadium electron has non-zero spontaneous magnetization, antiparallel to the magnetic order of Mn electrons. Below T_1^* the reoriented magnetic orders set in, which explains the increase of the magnetization when the temperature approaches zero¹. The description of this case is more complicated and requires three magnetic orders to be involved.

The present theory of ferrimagnetism permits the formulation of phenomenological rules which enable the analysis of experimental results for more complicated systems without explicit calculations. For example, the three-spin systems have, most generally, three characteristic temperatures

¹ When the field is so strong that all vanadium electrons are reoriented, an anomalous increase of magnetization below T^* would be obtained.

$T_1^* < T_2^* < T_N$. The Neel temperature T_N is the temperature at which the magnetic order sets in. When $T_2^* < T < T_N$ only one of the spins has non-zero spontaneous magnetization and the magnetization of the system equals the magnetic order of that spin. When $T_1^* < T < T_2^*$ two of the spins contribute to the magnetization of the system. If $M(T_2^*)$ is the local maximum the two spins are antiparallel. If the magnetization shows an anomalous enhancement below T_2^* the two spins are parallel. Below T_1^* all three spins have non-zero spontaneous magnetization, and the magnetization changes slope at this temperature.

As an example I consider the CeCrSb₃ compound [20]. The magnetic behavior is determined by Cr ions and Ce-4f electrons, which are located in different sublattices. The strong anisotropy leads to different curves of magnetization along different axes. The measurements of the magnetization and electric resistivity on a single crystal of CeCrSb₃ along the *c* axis show that there are three characteristic temperatures, the Neel temperature $T_N = 115$ K, $T_2^* = 108$ K, at which the magnetization is maximal, and $T_1^* = 18$ K, at which the magnetization is minimal. The closeness of T_N and T_2^* leads to misinterpretation and even to misidentification of these temperatures, but an evident increase of magnetization when $T_2^* < T < T_N$ and subsequent decrease below T_2^* proves that there are three characteristic temperatures. Below T_1^* the magnetization increases again. The experimental results suggest that there are three magnetic orders. Part of the itinerant Cr electrons start to form magnetic order at the Neel temperature T_N and the rest at T_1^* , while the localized Ce-4f electrons do this at T_2^* ($T_2^* = T_{Ce}$). The field cooled magnetization curves depends on the field. An increasing field leads to an increase of the maximal value of the magnetization and to an increase of the zero temperature value of the magnetization. This shows that the applied field is parallel to the magnetic orders of chromium electrons. Finally, the temperature variation of the resistivity shows anomalous behavior at T_N and T_1^* . It is known [8] that the onset of magnetism in the itinerant systems is accompanied by a strong anomaly in resistivity. Hence, one can associate

these temperatures with the temperatures at which the itinerant chromium electrons start to form magnetic order.

Acknowledgment

The author wishes to thank Professor Suzuki for valuable discussions.

References

- [1] Neel L 1948 *Ann. Phys.* **3** 137
- [2] Wolf W P 1961 *Rep. Prog. Phys.* **24** 212
- [3] Buschow K H J 1980 *Handbook of Magnetic Materials* vol 1, ed E P Wohlfarth (Amsterdam: North-Holland) p 297
- [4] Gilleo M A 1980 *Handbook of Magnetic Materials* vol 2, ed E P Wohlfarth (Amsterdam: North-Holland) p 1
- [5] Van Stapele P P 1982 *Handbook of Magnetic Materials* vol 3, ed E P Wohlfarth (Amsterdam: North-Holland) p 603
- [6] Belov K P 1996 *Usp. Fiz. Nauk* **166** 669
Belov K P 1996 *Phys.—Usp.* **39** 623 (Engl. Transl.)
- [7] Kaplan H 1952 *Phys. Rev.* **88** 121
- [8] Craig P P, Goldberg W I, Kitchens T A and Budnick J I 1967 *Phys. Rev. Lett.* **19** 1334
- [9] Takahashi M 1986 *Prog. Theor. Phys. Suppl.* **87** 233
- [10] Takahashi M 1987 *Phys. Rev. Lett.* **58** 168
- [11] Karchev N 2008 *Phys. Rev. B* **77** 012405
- [12] Pfeleiderer C and Huxley A D 2002 *Phys. Rev. Lett.* **89** 147005
- [13] Verwey E J W 1939 *Nature* **144** 327
- [14] Belov K P 1993 *Usp. Fiz. Nauk* **163** 53
Belov K P 1994 *Phys.—Usp.* **37** 563 (Engl. Transl.)
- [15] Walz F 2002 *J. Phys.: Condens. Matter* **14** R285
- [16] Garcia J and Subias G 2004 *J. Phys.: Condens. Matter* **16** R145
- [17] Adachi K, Suzuki T, Kato K, Osaka K, Takata M and Katsufuji T 2005 *Phys. Rev. Lett.* **95** 197202
- [18] Carlea V O, Jin R, Mandrus D, Roessli B, Huang Q, Miller M, Schultz A J and Nagler S E 2007 *Phys. Rev. Lett.* **100** 066404
- [19] Baek S-H, Choi K-Y, Reyes A P, Kuhns P L, Curro N J, Ramachandran V, Dalal N S, Zhou H D and Wiebe C R 2007 *Preprint* 0707.0018
- [20] Jackson D D, McCall S K, Karki A B and Young D P 2007 *Phys. Rev. B* **76** 064408